ELSEVIER

Contents lists available at ScienceDirect

# **Inorganic Chemistry Communications**

journal homepage: www.elsevier.com/locate/inoche



# Research Article

# Ag nanoparticles supported on phosphate-layered double hydroxide: A sustainable catalyst for p-nitrophenol reduction and antimicrobial performance

Zineb Tchorbo<sup>a</sup>, Marieme Kacem<sup>a</sup>, J.M. Doña Rodriguez<sup>b</sup>, Meryem Idrissi Yahyaoui<sup>c</sup>, Abderrahim Essaddek<sup>a</sup>, Mounsef Neffa<sup>c</sup>, Abdeslam Asehraou<sup>c</sup>, Mustapha Dib<sup>a,\*</sup>

### ARTICLE INFO

### Keywords: Functionalized LDH Physicochemical investigation p-Nitrophenol reduction Antimicrobial properties Catalytic performance

### ABSTRACT

Silver nanoparticles were effectively supported on phosphorylated layered double hydroxide (Phos-LDH) using a simple and efficient synthesis approach. The resulting AgNPs/Phos-LDH composite was thoroughly characterized using spectroscopic, structural, morphological, and textural techniques to investigate its physicochemical properties and confirm the successful formation of the AgNPs/Phos-LDH nanocomposite. This latter exhibited excellent catalytic activity for the reduction reaction of p-nitrophenol to p-aminophenol, achieving a high conversion rate up to 95 % in a short reaction time (6 min). This efficient transformation highlights the catalyst's strong potential for environmental remediation. In addition to their catalytic properties, all samples were evaluated for their antimicrobial activity. The antimicrobial performance was assessed using four bacterial species and four fungal strains. The AgNPs/Phos-LDH composite exhibited the highest antimicrobial efficacy, as reflected by its lowest minimum inhibitory concentration values, demonstrating MIC as low as 2.6 mg/mL and 6.6 mg/mL for antibacterial and antifungal activities, respectively. The synergistic effect between phosphory-lated MgAl-LDH and silver nanoparticles contributed to the enhanced antimicrobial performance. These results reveal the strong antimicrobial activity of the AgNPs/Phos-LDH nanocomposite against a potentially wide range of pathogens, underscoring its promise as an effective antimicrobial agent.

# 1. Introduction

There are many pathogenic microorganisms, which are common sources of disease and infection in humans and animals [1,2]. To fight these microorganisms, numerous research teams are working hard to develop new, powerful, and cost-effective antimicrobial agents [3–5]. Recently, bioactive materials and functional materials have received a great deal of attention owing to their antimicrobial efficiency agents against microorganisms [6–8]. Furthermore, thanks to their various multifunctional and biological benefits, these antibacterial agents have found wide application in the biomedical field, including dental composite restorations [9], treatment of bacterial infections [10], food packaging [11,12] foot and mouth disease [13], agents delivery system

[14], ...etc. Furthermore, silver nanoparticles are widely regarded as highly effective and cost-efficient antibacterial agents capable of eliminating large populations of bacteria [15]. However, they are chemically and thermodynamically unstable, and their tendency to aggregate due to high surface activity reduces dispersion and stability, thereby markedly diminishing their antibacterial efficacy [16]. The immobilization of silver Nanoparticles into other material surfaces provides an opportunity to overcome the clustering and transformational limitations associated with these nanomaterials. [17]. Additionally, In the field of catalysis, many rare metals such as rhenium, palladium, platinum and gold have been widely used for the reduction of nitroaromatic compounds [18,19]. More than, these catalysts present a number of features, in particular their high cost and their potentially harmful effects on the

E-mail address: d.mustapha@ump.ac.ma (M. Dib).

a Laboratory of Applied Chemistry and Environment, Mineral Solid Chemistry Team, Faculty of Sciences, Mohammed Premier University, B.P. 717, 60 000, Oujda,

<sup>&</sup>lt;sup>b</sup> Grupo de Fotocatálisis y Espectroscopía para Aplicaciones Medioambientales (FEAM), Institute of Environmental Studies and Natural Resources (i-UNAT), Universidad de Las Palmas de Gran Canaria, 35017, Spain

c Laboratory of Bioresources, Biotechnology, Ethnopharmacology and Health, Faculty of Sciences, Mohammed Premier University, B, P, 717, Oujda 60000, Morocco

<sup>\*</sup> Corresponding author.

environment and health [20]. The development of new alternative catalysts that are less costly, more efficient and more environmentally friendly is therefore a major challenge for scientific research [21]. Layered double hydroxide (LDH) compounds, which are also named hydrotalcite or anionic clays, are mesoporous crystalline layered materials featuring positively charged layers balanced by intercalated anions. Such materials are typically supplied according to the standard formula  $[M^{2+}_{(1-x)}M_x^{3+}(OH)_2]^{x+}$  (A<sup>n-</sup>)<sub>x/0</sub>·mH<sub>2</sub>O, where m corresponds to the hydration degree, often equal to 4. M<sup>2+</sup> (Mg, Ba, Cu, Ca, Co, Ni, or Zn...) and M<sup>3+</sup> (Cr, Fe, or Al..) designate di- and trivalent cations respectively. The intercalated anions (A<sup>n-</sup>) commonly include CO<sub>3</sub><sup>2-</sup>, Cl<sup>-</sup>, NO<sub>3</sub><sup>-</sup>, or PO<sub>4</sub><sup>3-</sup> (Fig. 1). However, metal cations and anions compounds can be substituted with a variety of alternatives, leading to improved physicochemical properties of the LDH materials. Owing to their structural versatility and ion-exchange capacity, hydrotalcite-based compounds have been widely applied in diverse fields, particularly in heterogeneous catalysis for heterocyclic synthesis [22-25], biomedical and medicine [26], agricultural technology [27], energy [28], environment and water treatment [29-31].

In addition, the LDH materials most frequently studied or commercialized have been produced by co-precipitation, hydrothermal treatment or a combination of the two techniques. All three processes produce a well-crystallized product with good reproducibility, but require lengthy hydrothermal aging [32]. Among these, lamellar materials have recently attracted significant interest as promising multifunctional nanomaterials due to their unique structure and extraordinary properties [33]. To design optimal and effective antimicrobial agents, it is essential to consider functional and realizable materials. Furthermore, several strategies have been explored to develop effective antimicrobial agents [34]. Kotta et al [35] developed silver nanoparticles (AgNPs) enrobed with LDH material for delivery in a polymer hydrogel as potential antimicrobial agents. After the successful use of gold nanoparticles confined in a porous silica network in the reduction of 4-nitrophenol [36], which is considered a harmful pollutant that impacts human health as well as the ecological system, to aminophenol which is a precursor commonly used in the pharmaceutical industry, we were interested in providing a detailed survey in this study of the catalytic behavior of silver nanoparticles decorated on the surface of phosphorylated-LDH structure, leading to unexpected results significantly outstripping the results previously obtained with gold nanoparticles, considerably more costly compounds compared with silver, vielding substantially improved conversion times and vields. In this work, we focused on developing a novel phosphate-functionalized

layered double hydroxide (Phos-LDH) decorated with silver nanoparticles (AgNPs/Phos-LDH) and investigating its physicochemical properties. The Phos-LDH support not only enhances the dispersion and stabilization of Ag<sup>0</sup> nanoparticles but also improves catalytic activity and antimicrobial efficiency, highlighting its potential as a sustainable multifunctional material.

# 2. Experimental

### 2.1. Preparation of LDH

The LDH material produced was successfully achieved following a co-precipitation process [37,38]. In brief, solution (A) containing 0.15 M of Mg(NO<sub>3</sub>)<sub>2</sub>·6H<sub>2</sub>O and 0.05 M of Al(NO<sub>3</sub>)<sub>3</sub>·9H<sub>2</sub>O with an Mg/Al ratio of 3:1, and another solution (B) containing 0.4 M of NaOH and 0.025 M of Na<sub>2</sub>CO<sub>3</sub>, were prepared separately. The two solutions were added simultaneously dropwise into a Three-neck round-bottom flask maintained at 60 °C under continuous stirring and the pH was maintained at 10. The resulting mixture was then heated to reflux at 75 °C for 18 h. The precipitate was filtered, washed with distilled water, and dried at 80 °C overnight.

### 2.2. Preparation of Phos-LDH

The Phos-LDH composite was synthesized following the procedure reported by He et al. [39], with minor modifications. First, 1.4 g of LDH was dried at 120 °C for 1 h and then dispersed in a mixture of ethanol (15 mL) and water (10 mL) under continuous stirring for 30 min. Subsequently, 3 mL of triethyl phosphate (( $C_2H_5)_3PO_4$ ) was added dropwise to the suspension under stirring, and the mixture was maintained at room temperature for 24 h. Afterward, 6 mL of distilled water was added, followed by an additional 2 h of continuous stirring. The resulting precipitate was filtered, thoroughly rinsed with distilled water and ethanol, and then dried at 80 °C for 24 h (Fig. 2).

# 2.3. Preparation of AgNPs/Phos-LDH

The AgNPs/Phos-LDH composite was synthesized by dissolving 0.30 g of AgNO<sub>4</sub> in a mixture of distilled water (100 mL) and ethanol (50 mL), followed by suspending 300 mg of Phos-LDH in the prepared solution. Subsequently, 0.03 M NaBH<sub>4</sub> was added, and the pH was adjusted to 9 using 1 M of NaOH. The mixture was then heated under reflux at 60  $^{\circ}\text{C}$  for 17 h. After the reaction, the product was filtered, thoroughly washed

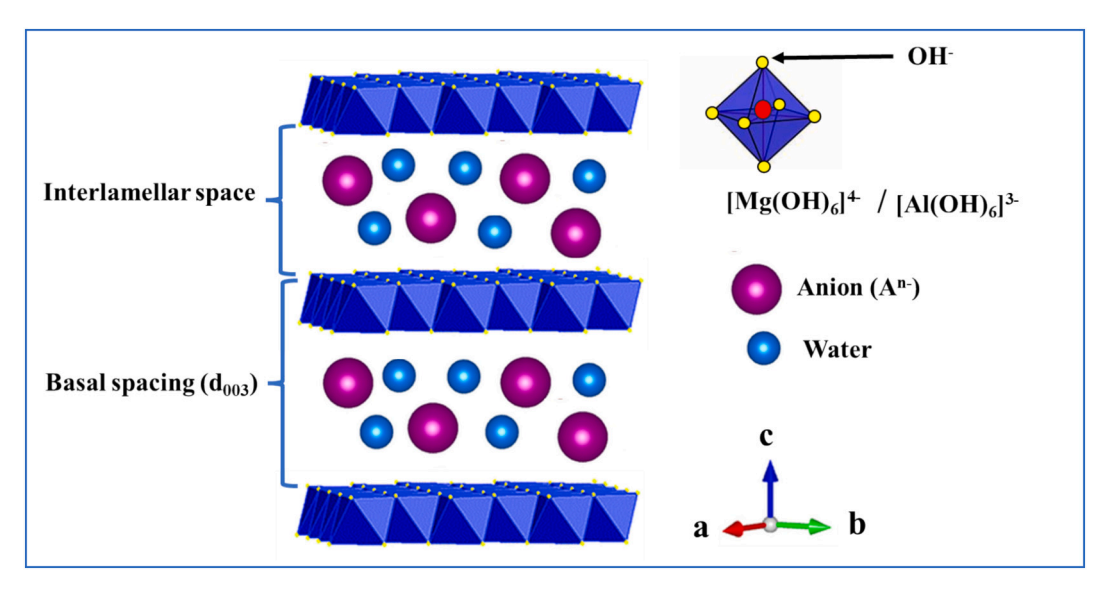


Fig. 1. MgAl-Layered double hydroxide structure.

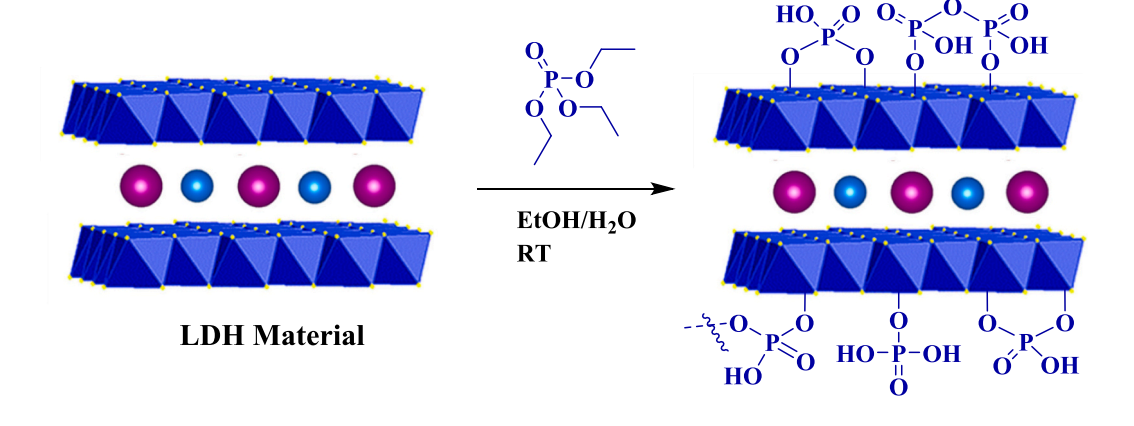


Fig. 2. Schematic Representation of Surface Phosphorylation of LDH

with ethanol, and dried in an oven at 60 °C (Fig. 3).

# 2.4. In vitro testing of antimicrobial activity

### 2.4.1. Bacterial strains

In this study, we used four bacterial strains, including *E. coli* (ATCC 10536), *S. aureus* (ATCC 6538), *P. aeruginosa* (ATCC 15442), and *M. luteus* (ATCC LP 14110), as model micro-organisms to evaluate the antibacterial efficacy of all the synthesized materials. These bacterial strains were obtained from the MBBT laboratory, FS, UMP Oujda, Morocco [40].

# 2.4.2. Fungal strains

In this study, we chose four distinct fungal strains, including *A. niger*, *R. glutinis*, *C. glabrata* and *P. digitatum*, to evaluate the antifungal performance of the composites. These fungal strains were obtained from the MBBT laboratory, FS, UMP Oujda, Morocco [41].

# 2.4.3. Determination of MIC

Determination of the minimum inhibitory concentration (MIC) is a very important step in assessing the efficacy of antimicrobial agents. This study used the resazurin microtiter assay to establish the MIC of the compounds studied. The test was performed in 96-well microplates, each containing a concentration ranging from 15 mg/mL to 0.05 mg/mL. A standardised inoculum of the microbial strain was introduced into

each well and the microplates were incubated at the appropriate temperature, 37  $^{\circ}$ C for bacteria and 25  $^{\circ}$ C for fungi, for 18 h. After incubation, resazurin was added and the microplates were incubated for 2 h until a colour change from blue to pink was observed [42].

**Phos-LDH** composite

### 3. Results and discussion

### 3.1. IR Analysis

The FT-IR spectra of the LDH, LDH-Phos and AgNPs/Phos-LDH samples can be viewed in Fig. 4, revealing the variations in structure and composition seen in the native and functionalised materials. For the LDH material, the wide band around 3400 cm<sup>-1</sup> reflects the O—H bond stretching frequencies typically associated with hydroxyl and water molecules in the LDH structure, [43]. The wide, moderately intense band at 1362 cm<sup>-1</sup> is attributed to the vibrational modes of the intercalated carbonate group (CO<sub>3</sub><sup>2-</sup>), a characteristic anion of LDH. Other bands in the lower wavenumber region ( $\sim$ 600 cm<sup>-1</sup>) arise from bending vibrations of metal-oxygen bonds, reflecting metal hydroxide groups. In the LDH-Phos spectrum, a notable shift in the O-H stretching band is observed, indicating interactions between hydroxyl groups and phosphate species. The band at 1362 cm<sup>-1</sup> persists, reaffirming the presence of carbonate ions, but the appearance of a new band in the 700-800 cm<sup>-1</sup> range corresponds to P—O and P=O stretching vibrations. This confirms the successful functionalization of LDH by the phosphate

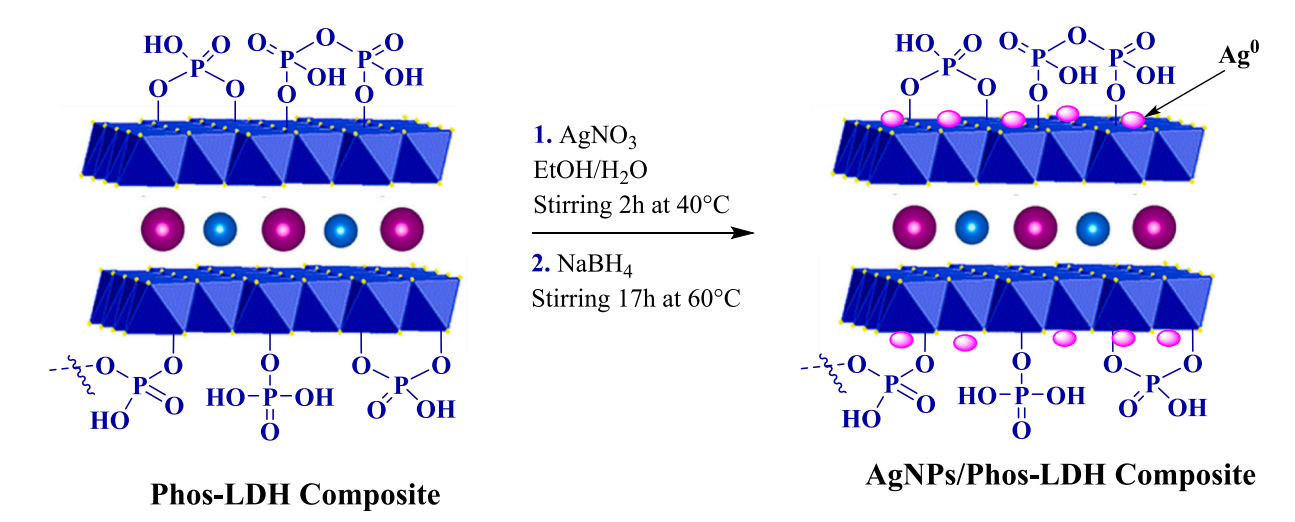


Fig. 3. Schematic representation of Ag nanoparticles anchoring onto the surface of phosphorylated LDH.

groups [44]. Finally, the AgNPs/Phos-LDH composite retains the characteristic hydroxyl and phosphate bands, although with reduced transmission intensities. Such reduction is mainly explained by the inclusion of silver nanoparticles, which probably interfered with the vibrational modes due to their interaction with the phosphate-functionalised LDH composite. The spectral features collectively confirm the successful integration of phosphate groups and silver nanoparticles into the LDH structure.

### 3.2. XRD characterization

The XRD patterns of the LDH, and LDH-Phos samples (see Fig. 5), depict reflections at  $11.33^\circ, 22.82^\circ, 34.42^\circ, 38.23^\circ, 60.39^\circ$  and  $61.67^\circ$ typically related to the LDH lamellar structure corresponding to the (003), (006), (012), (015), (018), (110) and (113) crystal planes, as reported in JCPDS file no. 41-1428 [45]. In the case of Phos-LDH, a shift in the 20 position of reflection (003) and a slight variation in d-spacing indicate that the successful intercalation of phosphate anions into the LDH structure via anion exchange has not been accomplished. However, the XRD patterns suggest that surface functionalization of the LDH with phosphate groups, without true intercalation likely occurred, although the fundamental layered structure of LDH remains intact [46,47]. In the NPs/Phos-LDH diffractogram, similar LDH phase patterns with additional peaks appearing at 27.94°, 38.27°, 44.38° and 77.55°, corresponding to the (220), (111), (200) and (311) planes of the Ag nanoparticles (JCPDS file no. 04-0783) [48]. The results suggest the successful deposition of silver nanoparticles onto the phosphatefunctionalized LDH framework. Table 1 lists the crystallite sizes estimated using Scherrer's formula (Eq. 1) and the d-spacing.

$$D = 0.9\lambda/\beta^* \cos(\theta) \tag{1}$$

### 3.3. N<sub>2</sub> adsorption-desorption

Fig.6 presents the  $N_2$  adsorption and desorption isotherms of LDH, Phos-LDH and AgNPs/Phos-LDH using BET method. Both samples demonstrate type IV isotherms, characteristic of mesoporous materials, confirming the presence of a well-defined porous structure [49]. The

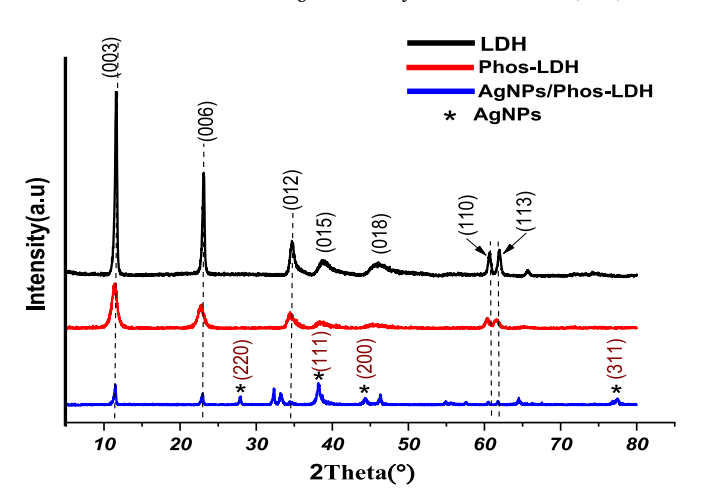


Fig. 5. XRD patterns of LDH, Phos-LDH, and AgNPs/Phos-LDH.

surface modification of the LDH material by phosphorylation results in a significant increase in specific surface area from 79.52 to  $102.57~\text{m}^2/\text{g}$  for LDH and Phos-LDH, respectively (Fig.6). This enhancement is probably due to interactions between phosphate groups and LDH layers. Furthermore, the decoration of phosphorylated LDH with silver nanoparticles involves a minor enhancement of surface area and pore volume. Consequently, functionalization of the LDH surface can induce structural modifications.

# 3.4. Morphological and microstructural analyses

### 3.4.1. SEM/EDS analysis

SEM combined with EDS was employed to examine the microstructural properties, surface morphology, and elemental distribution of the samples (LDH, Phos-LDH and AgNPs/Phos-LDH) as presented in Figs. 7,8,9 and Fig. S1. In Fig. 7 (a) and Fig. 8, the LDH sample shows coarse, irregularly distributed particles with diameters ranging from around 1.2 to 5.1  $\mu m$ . These observations confirm the presence of a three-dimensional lamellar structure with a characteristic hexagonal

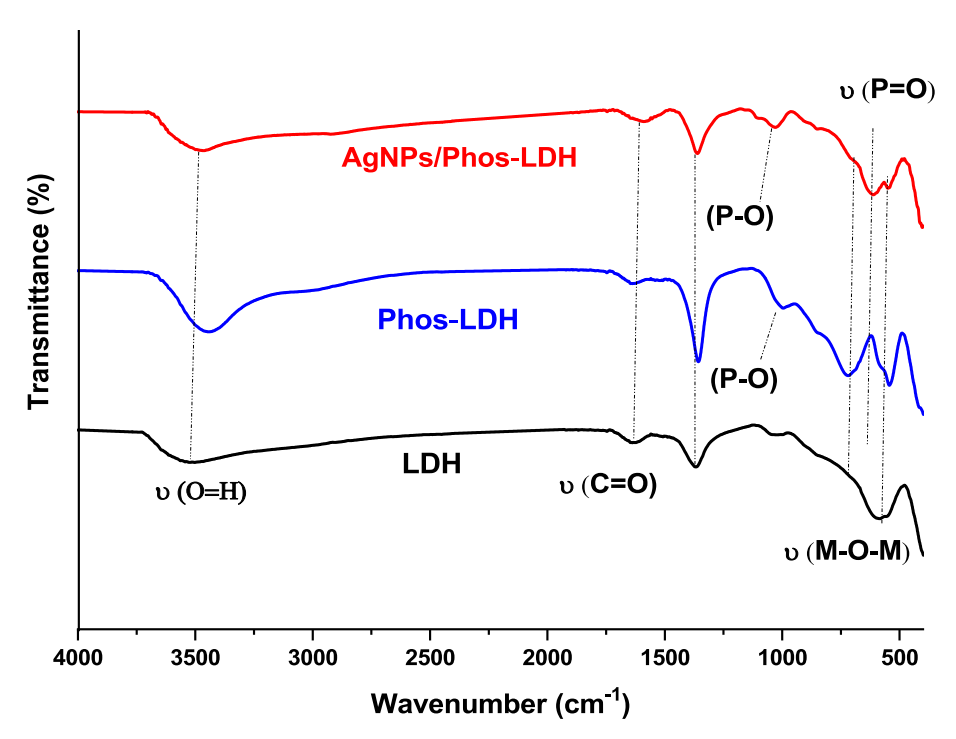


Fig. 4. FTIR spectra of LDH, Phos-LDH, and AgNPs/Phos-LDH.

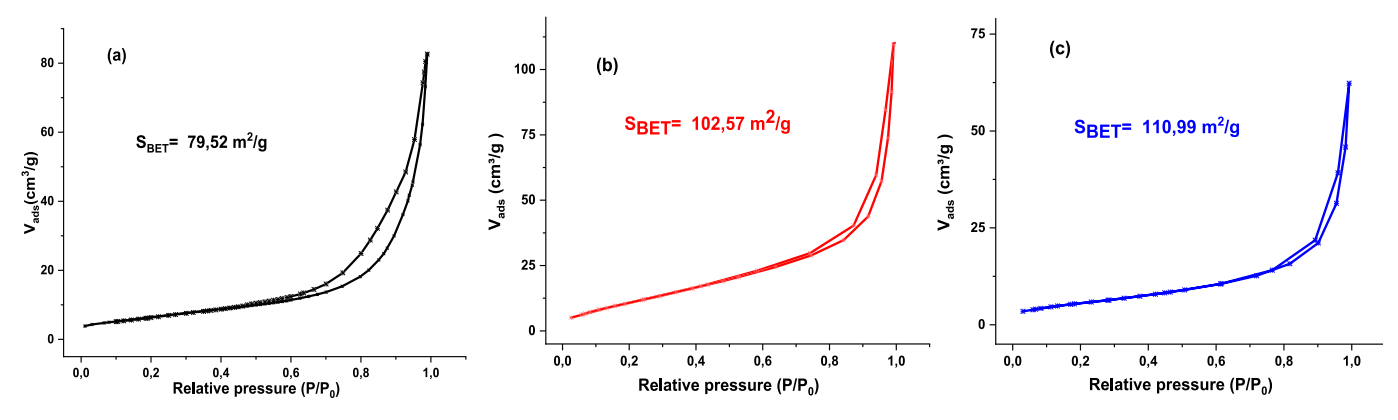


Fig. 6. N<sub>2</sub> Adsorption-desorption isotherms of LDH (a), Phos-LDH (b), and AgNPs/Phos-LDH (c).

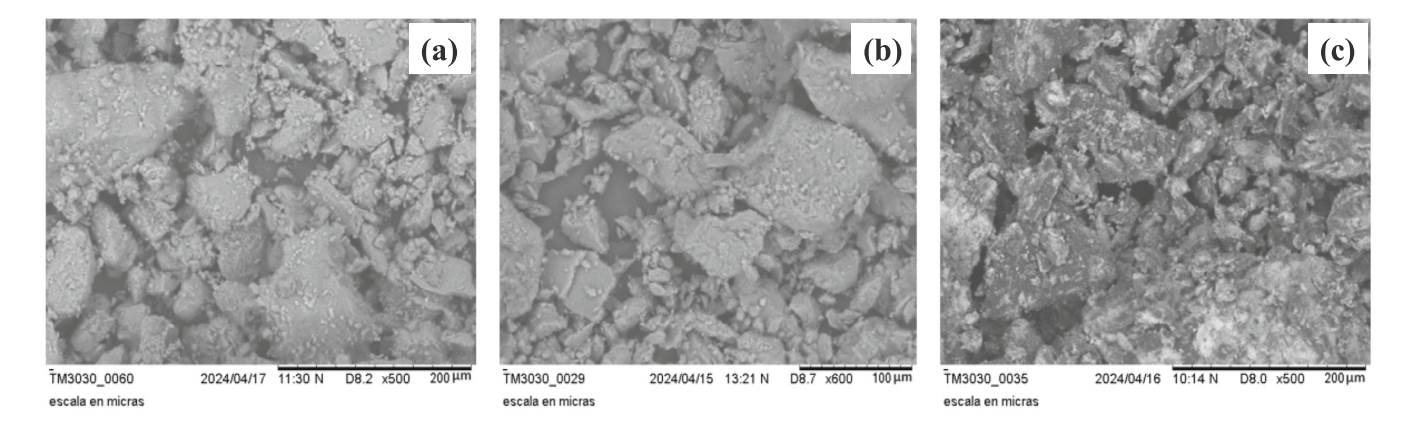


Fig. 7. Images SEM of the samples: LDH (a), Phos-LDH (b) and Ag NPs/ Phos- LDH (c).

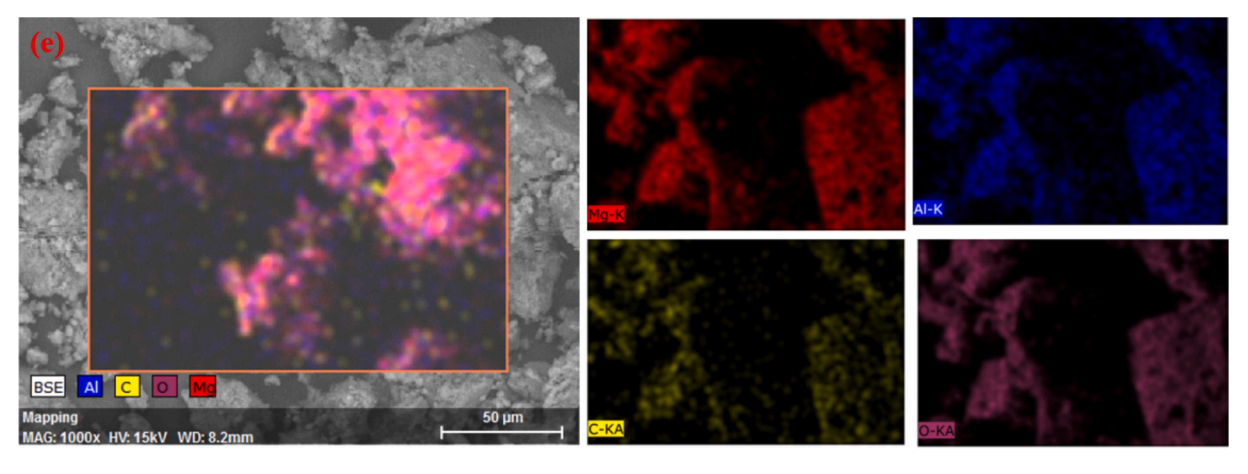


Fig. 8. SEM-EDS elemental mapping of LDH Material, image and analogous elemental mapping of Mg, Al, O, and C.

morphology [50].

Fig. 7(b) and Fig. 9 reveals a notable transformation in particle morphology for Phos-LDH. Particle size varies from 3.1 to 5.2  $\mu m$ , and the material exhibits more defined and homogeneous characteristics. The appearance of smaller, evenly dispersed particles suggests that the phosphate groups effectively coated the LDH surface, leading to better particle dispersion and structural uniformity.

In contrast, Fig. 7(c) and Fig. 10 shows particles of similar size for AgNPs/Phos-LDH, but with distinct bright spots visible on the surface. These bright regions correspond to the presence of silver nanoparticles, as confirmed by EDS analysis. The uniform distribution of these

nanoparticles indicates successful deposition on the phosphate-functionalized LDH material, enhancing the surface properties of the composite. The results of the SEM and EDS analyses collectively demonstrate that the modifications involving phosphate and silver nanoparticles were executed efficiently, leading to increased material uniformity and successful integration of the functional groups and nanoparticles.

# 3.4.2. TEM analysis

Fig. 11 presents the HRTEM images of the synthesized materials. Theimage Fig. 11(a) shows the characteristic morphology of LDH

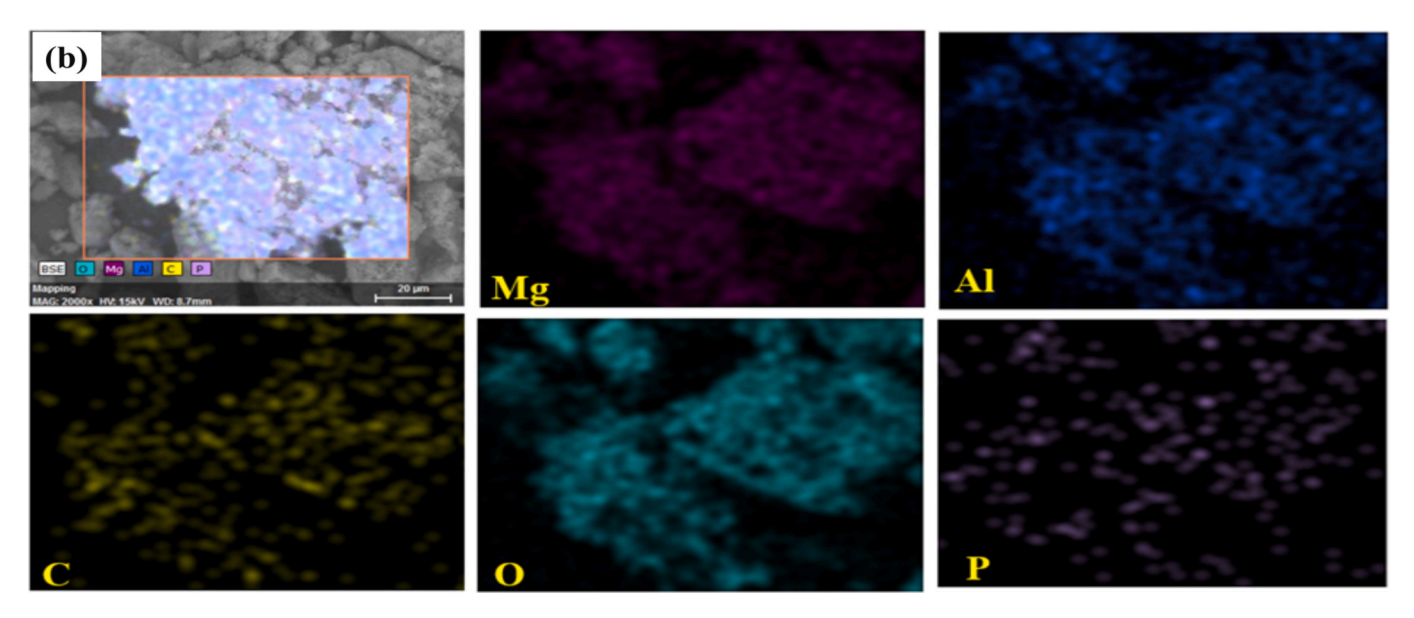


Fig. 9. SEM-EDS elemental mapping of Phos-LDH, image and analogous elemental mapping of Mg, Al, O, C and P.

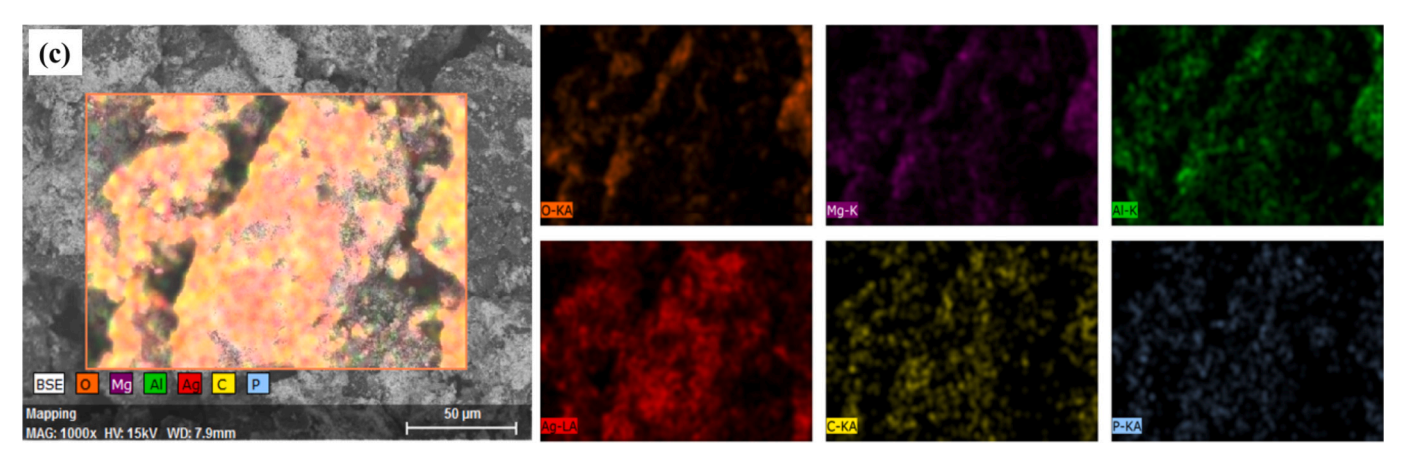


Fig. 10. SEM-EDS elemental mapping of AgNPs/Phos-LDH, image and analogous elemental mapping of Mg, Al, O, C, P and (Ag).

material before phosphorylation by phosphate groups. It shows a structure of thin, superimposed, well-defined layers, typical of the lamellar nature of these materials. This stacked layer organization reflects the good crystallinity and orderly structure of the LDH material. Fig. 11(b) illustrates the morphology of the phosphorylated LDH. Partial exfoliation of the layers can be observed, reflecting a disruption of the initial lamellar structure due to functionalization by phosphate groups. These groups appear to attach themselves to the surface of the platelets, thereby modifying the stacking and contributing to a more pronounced dispersion of the layers. Fig. 11(c) exhibits the morphology and distribution of silver nanoparticles supported by a phosphorylated layered double hydroxide (Phos-LDH). The AgNPs are mainly spherical to quasispherical in shape, with sizes ranging from approximately 30 to 40 nm. These nanoparticles appear to be well dispersed in the Phos-LDH support, with no significant aggregation observed, indicating efficient deposition and good interaction with the support surface.

Fig. 11 shows HRTEM images of the synthesized materials. Fig. 11(a) shows the characteristic morphology of the native LDH material. A structure composed of thin, superimposed, well-defined layers, typical of the lamellar nature of LDH, can be observed. This arrangement reflects good crystallinity. and ordered structure of the material. Fig. 11(b) illustrates the morphology of phosphorylated LDH (Phos-LDH). Partial exfoliation of the layers is evident, indicating a disruption of the original lamellar structure due to functionalization with phosphate groups.

These groups appear to attach to the surface of the platelets, thereby altering the stacking and promoting greater dispersion of the layers. Fig. 11(c) shows the morphology and distribution of silver nanoparticles supported on Phos-LDH composite. The AgNPs are mainly spherical to quasi-spherical, with sizes ranging from approximately 30 to 40 nm. They are well dispersed on the Phos-LDH support, with no significant aggregation observed, suggesting efficient deposition and strong interaction with the support surface.

Fig. 11(d) shows an HRTEM image of the AgNPs/Phos-LDH composite revealing sharp, well-parallel lattice fringes over large areas, providing direct evidence of the composite's crystalline nature. The presence of differently oriented grains confirms the composite's polycrystalline structure. Furthermore, certain weakly structured or disordered areas can be attributed to amorphous phases or the presence of crystalline defects.

Fig. 11 (e) shows electron diffraction by a ring for the AgNPs/Phos-LDH composite. This type of image is essential for microstructural analysis, particularly for assessing the degree of crystallinity and identifying the crystalline phases present. In our case, the presence of well-defined concentric rings indicates a polycrystalline structure of the composite. These rings are likely associated with both silver nanoparticles and sheets of phosphorylated lamellar material, reflecting the coexistence of different crystalline phases in the sample.

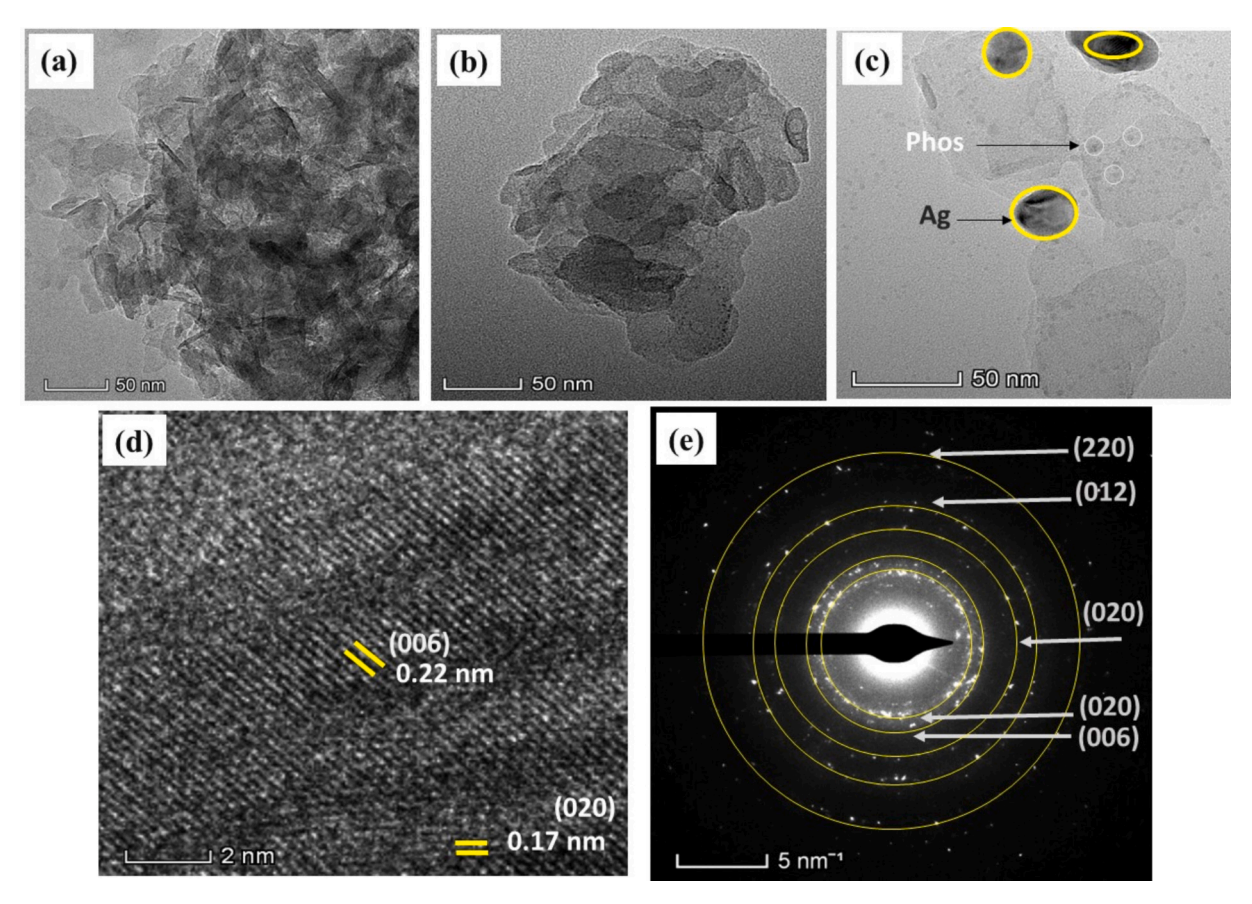


Fig. 11. TEM images of LDH (a), Phos-LDH (b) AgNPs/Phos-LDH (c), HRTEM of AgNPs/Phos-LDH (d) and SAED of AgNPs/Phos-LDH (e).

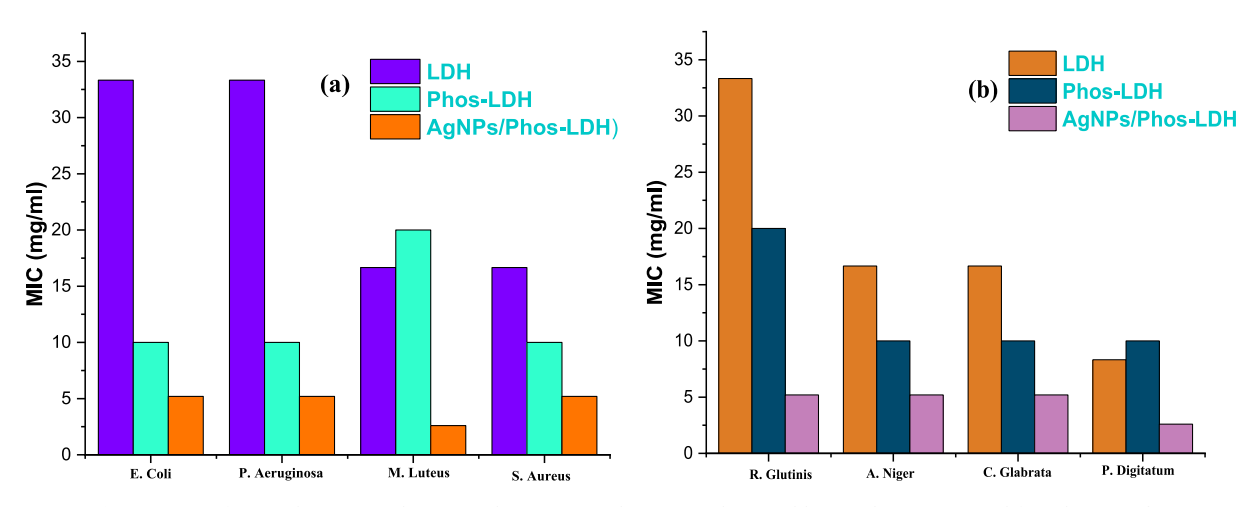


Fig. 12. MIC of LDH, Phos-LDH and Ag NPs/Phos-LDH samples against the tested bacterial strains (a) and fungal strains (b).

# 4. Antimicrobial activity

# 4.1. Antibacterial activity

The antibacterial properties of LDH, Phos-LDH and the newly composite AgNPs//Phos-LDH were assessed by determining their minimum inhibitory concentration (MIC) using standard dilution methods [51].. For example, LDH material showed MIC values of 16.66 mg/mL against *M. luteus* and 33.33 mg/mL against *E. coli*, while AgNPs/Phos-LDH showed MIC values of 2.60 mg/mL against *M. luteus* and 5.20 mg/mL against *E. coli*. These results suggest that Ag-decorated Phos-LDH exhibits superior antibacterial activity to LDH and Phos-LDH. As a result,

Phos-LDH and AgNPs/Phos-LDH exhibit considerable antimicrobial activity against a wide range of bacterial and fungal strains tested (Fig. 12 (a)). The data were statistically analyzed using IBM SPSS Statistics V21.0 software, with descriptive statistics used to present the results as mean  $\pm$  SD. An analysis of variance (ANOVA) was conducocted to compare the mean values of the studied characteristics, followed by Tukey's post-hoc test to determine significant differences at a 5 % threshold (Table 3 and Table 4). The MIC values of antibacterial activity for each compound and statistical data were presented in the Table 3.

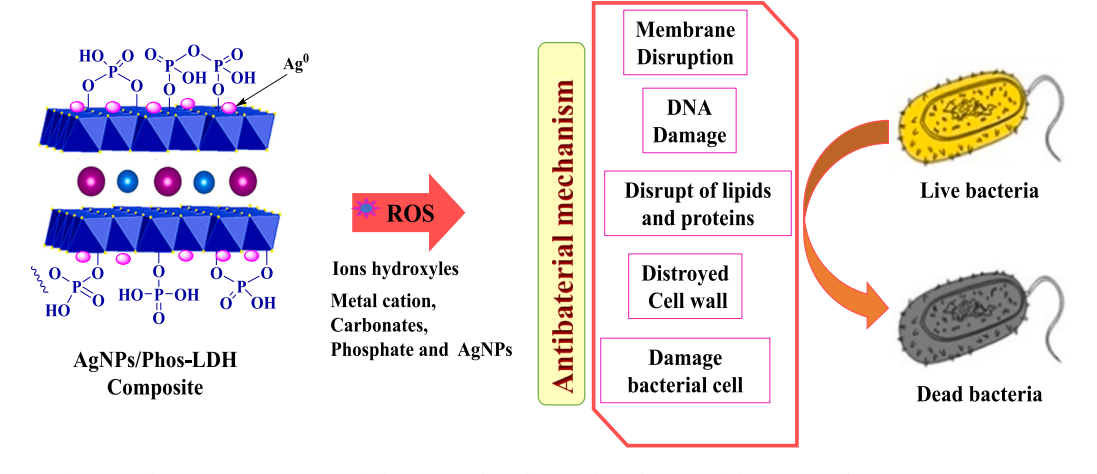


Fig. 13. Schematic representation of the proposed antibacterial mechanism of the AgNPs/ Phos-LDH nanocomposite.

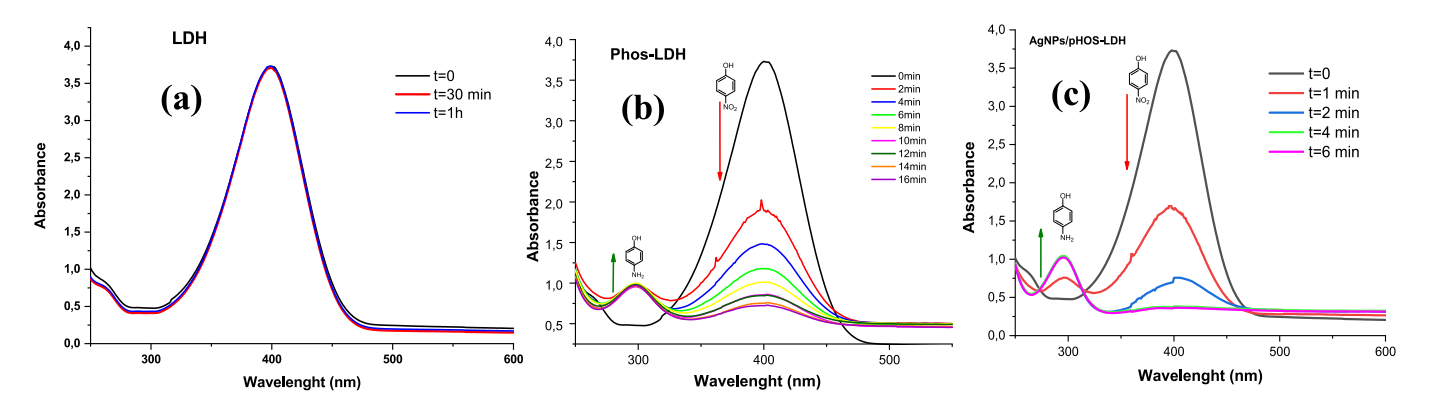


Fig. 14. UV-Visible spectra of p-NP in the presence of LDH (a), Phos-LDH (b) and AgNPs/Phos-LDH catalyst;

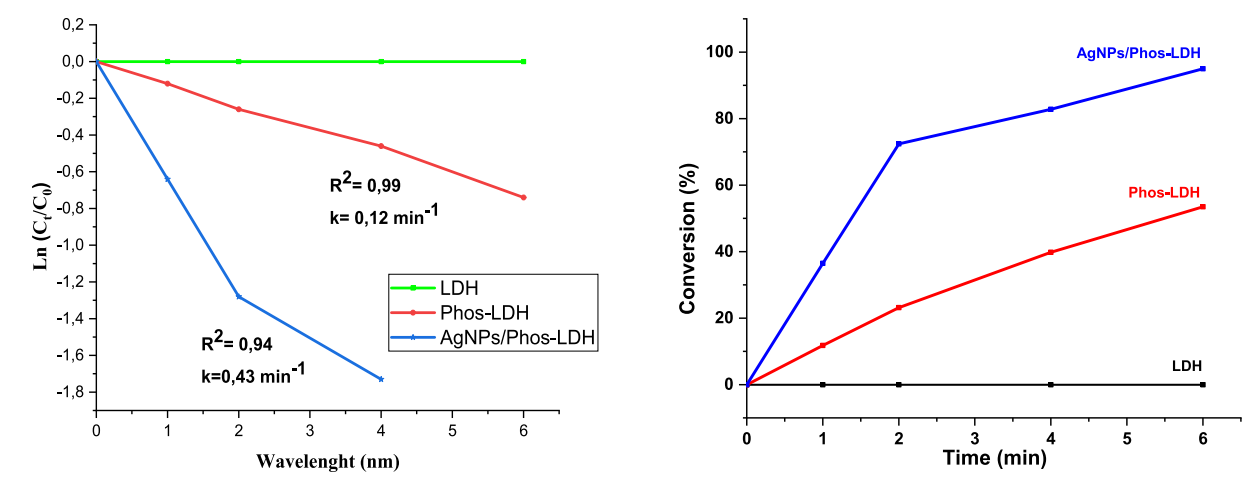


Fig. 15. Rate constants of p-NP and conversion of catalysts.

# 4.2. Antifungal activity

In the second antimicrobial assay, the antifungal activity of LDH, Phos-LDH and AgNPs/Phos-LDH composites was evaluated against four fungal strains including *P. digitatum*, *A. niger*, *C. glabrata* and *R. glutinis* for determining their MIC values (Table 4). The new AgNPs/Phos-LDH composite exhibited the best antifungal activity for all the strains tested, with significantly lower MIC values (2.60–5.20 mg/mL) compared with LDH and Phos-LDH. In contrast, LDH showed the weakest antifungal effect, particularly against *R. glutinis* (33.33 mg/mL).

Phos-LDH showed moderate activity with uniform MIC values (10 mg/mL) for all strains. These results highlight the improved antifungal performance of the Ag-supported Phos-LDH composite, suggesting a synergistic action between the Ag nanoparticles and the phosphorylated LDH, which probably enhances the disruption of fungal cell membranes or interferes with their metabolic processes (Fig. 12(b)).

LDH materials are widely recognized for their biocompatibility, with their toxicity being largely influenced by their composition and interlayer anions [52]. Pattappan et al. [53] reported the versatility of phosphate-containing LDHs, emphasizing their favorable safety profiles

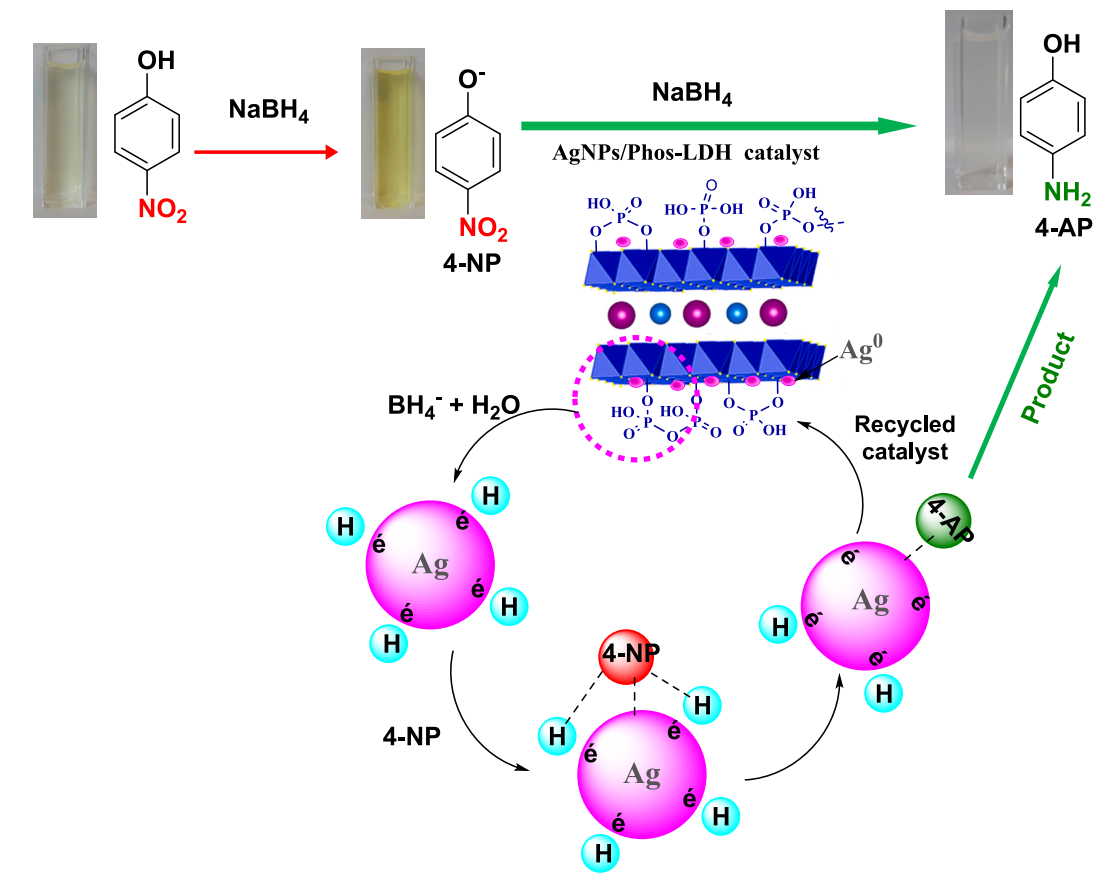


Fig. 16. Schematic illustration of the mechanism behind the catalyst AgNPs/Phos-LDH for the.

**Table 1** Estimation of crystallite size by Scherrer formula.

Sample	d <sub>(003)</sub> (Å)	Crystallite size (nm)
LDH	7807	29,9
Phos-LDH	7631	42,2
AgNPs/Phos-LDH	7690	61,4

**Table 3**Results of antibacterial activities and statistical data of results.

	Sample	Bacterial strains			
		Gram (+) bacteria		Gram	(–) bacteria
		S. aureus	M. luteus	E. coli	P. aeruginosa
100	LDH	$16.66 \pm 0.01^{cA}$	$16.66 \pm 0.00 ^{\text{cA}}$	$33.33 \pm 0.03 ^{\text{cB}}$	$\begin{array}{c} 33.33 \pm 0.06 \\ \text{\tiny cB} \end{array}$
MIC (mg/ ml)	Phos-LDH	$\begin{array}{c} 10.00 \pm \\ 0.09^{bA} \end{array}$	$10.00 \pm 0.03 ^{\ bA}$	$10.00 \pm 0.00 \ ^{bA}$	$10.00\pm0.01_{\text{bA}}$
	AgNPs/ Phos-LDH	$\begin{array}{l} 5.20 \; \pm \\ 0.00^{aB} \end{array}$	$\begin{array}{l} 2.60 \; \pm \\ 0.02 \end{array}$	$\begin{array}{l} 5.20~\pm \\ 0.04~^{aB} \end{array}$	$5.20\pm0.00~^{aB}$

Note: Values in the same column followed by different lowercase letters (a–c) are significantly different, while values in the same row followed by different uppercase letters (A–B) differ significantly at p<0.05. SD = Standard Deviation.

in both environmental and biomedical applications. In addition, metal oxide and silver nanoparticles may exhibit low toxicity, depending on dose and size, attributed in part to the stabilization of silver nanoparticles (Ag $^0$ ) [54–56]. As a result, these insights suggest that AgNP/Phos-LDH nanocomposites are promising candidates that combine functionality with reduced toxicity risk.

**Table 4** results of antifungal activities and statistical data of results.

	Sample		Funga	al strains		
		P. digitatum	A. niger	C. glabrata	R. glutinis	
MIC (mg/ ml)	LDH Phos-LDH AgNPs/ Phos-LDH	$8.33 \pm 0.00 \\ 10.00 \pm \\ 0.20 ^{\text{bA}} \\ 2.60 \pm 0.09 \\ \text{aA}$	$16.66 \pm \\ 0.00 ^{\text{CB}} \\ 10.00 \pm \\ 0.10 ^{\text{bA}} \\ 5.20 \pm \\ 0.10 ^{\text{aB}}$	$\begin{array}{c} 16.66 \pm \\ 0.10^{~cB} \\ 10.00 \pm \\ 0.10^{~bA} \\ 5.20 \pm 0.20 \\ ^{aB} \end{array}$	$\begin{array}{l} 33.33 \pm \\ 0.10^{\text{ eC}} \\ 10.00 \pm \\ 0.30^{\text{ bA}} \\ 5.20 \pm \\ 0.00^{\text{ aB}} \end{array}$	

### 4.3. Proposed antibacterial mechanism

Some studies showed that nanocomposites can interact electrostatically with bacterial membranes, leading to membrane rupture, inhibition of periplasmic enzymes and, ultimately, cell destruction [57]. The antimicrobial activity of layered double hydroxide (LDH) is mainly caused by the release of hydroxyl groups (OH-) into the aqueous solution. These highly reactive ions can oxidize and interact with various biomolecule compounds. The Phos-LDH functional material can also catalyze the generation of ROS, such as hydroxyl radicals, as well as carbonates and phosphate groups under physiological conditions. These ROS induce oxidative stress, leading to damage of bacterial cell walls and membranes. Furthermore, ROS can penetrate bacterial cells and further damage intra-cellular biomolecules such as lipids, DNA, and proteins. The incorporation of silver nanoparticles (AgNPs) into Phos-LDH enhances its antimicrobial activity by improving its stability and prolonging its effect. Silver nanoparticles specifically target bacterial components, such as enzymes and ribosomes, disrupting critical metabolic processes and amplifying the overall antibacterial effect (Fig. 13).

Several studies have shown that nanocomposites can interact

electrostatically with bacterial membranes, leading to membrane rupture, inhibition of periplasmic enzymes, and ultimately cell death [57]. The antimicrobial activity of LDH material is primarily attributed to the release of hydroxyl groups (OH<sup>-</sup>) into the aqueous medium. These highly reactive ions can oxidize and interact with various biomolecules. In addition, the Phos-LDH functional material can catalyze the generation of reactive oxygen species (ROS), such as hydroxyl radicals, carbonates, and phosphate-derived species under physiological conditions. These ROS induce oxidative stress, resulting in damage to bacterial cell walls and membranes. Moreover, ROS can penetrate bacterial cells and disrupt intracellular biomolecules, including lipids, DNA, and proteins. The decoration of Phos-LDH by silver nanoparticles (AgNPs) further enhances antimicrobial activity by improving stability and prolonging effectiveness. AgNPs specifically target bacterial components, such as enzymes and ribosomes, thereby disrupting critical metabolic processes and amplifying the overall antibacterial effect (Fig. 13).

# 5. Catalytic performance of AgNPs/Phos-LDH

# 5.1. Reduction reaction of p-NP

The catalytic performance of the synthesized nanocomposites was studied in the reduction reaction of para-nitrophenol in aqueous medium, using our previous procedure described by Kacem et al. [36]. In a typical experiment, 2 mg of the catalyst was added to a flask (10 mL) containing an aqueous solution of p-NP (0.2 mmol), followed by vigorous stirring for 2 min to ensure homogeneous dispersion. Subsequently, a freshly prepared aqueous solution of NaBH<sub>4</sub> (3.6  $10^{-2}$  mmol) was added to the reaction mixture with continuous stirring. The progress of the reduction reaction was monitored in real time by UV–vis spectroscopy to observe the decreased of the absorption band characteristic of p-NP and the appearance of a new characteristic absorption band corresponding to para-aminophenol (p-AP).

Upon the addition of NaBH4 to the p-NP solution, a characteristic band appears at ~400 nm, representing the nitrophenolate ion. Subsequent to the addition of the catalyst (Phos-LDH and AgNPs/Phos-LDH), the reduction reaction can be observed. Gradually, as the reduction reaction proceeds towards p-aminophenol (p-AP), this band decreases, while a new band may appear around ~300 nm, indicating that a new product has been formed. However, the native LDH material does not exhibit significant catalytic activity for the reduction reaction to p-NP (Fig. 14. (a)). The catalytic tests carried out also show that the Phos-LDH catalyst exhibits a moderate and slow catalytic activity, although not zero like that of native LDH, suggesting that modifying the LDH surface can improve the catalytic activity of the final material (Fig. 14. (b)). A rapid decrease in the absorption band at 400 nm was observed, with almost complete disappearance within 6 min. At the same time, a new absorption band appeared clearly at 300 nm, indicating the formation of p-AP (Fig. 14(c)). This demonstrates the high catalytic efficiency of the new AgNPs/Phos-LDH system. The presence of silver nanoparticles considerably enhances electron transfer, accelerating the reduction of p-NP to p-AP. This enhanced activity results from the synergistic interaction between the phosphate-functionalized LDH surface and the incorporated silver nanoparticles.

The rate constant (k) for the reduction of p-nitrophenol (p-NP) was determined using the following first-order kinetic equation:

$$ln(c_t/c_0) = -kt (2)$$

where  $C_0$  and  $C_t$  represent the concentrations of p-NP at the initial time and at a given reaction time t, respectively, and k (min $^{-1}$ ) is the apparent rate constant. Based on this kinetic model, the calculated values of k were  $0.12~\text{min}^{-1}$  and  $0.43~\text{min}^{-1}$  for the reduction reaction in the presence of Phos-LDH and AgNPs/Phos-LDH, respectively. As a result, the LDH catalyst is inactive in the reduction of p-NP. It does not possess the electronic properties or active sites required to facilitate electron

transfer between BH<sub>4</sub><sup>-</sup> and p-NP. A regular increase in conversion, reaching around 56 % after 6 min, due to phosphorylation, which improves the catalytic activity of the LDH material. Phosphorylation can introduce phosphate groups capable of modifying the polarity of the surface, improving dispersion of the reagents or introducing acidic sites (Fig. 15). Phos-LDH has moderate catalytic activity, but is insufficient for rapid or complete conversion. In the presence of AgNPs/Phos-LDH catalyst, the conversion reaches around 70 % in 2 min and over 95 % at 6 min. These results are due to the presence of silver nanoparticles (AgNPs) on the surface of Phos-LDH material act as highly active catalytic sites. They effectively facilitate electron transfer from BH $_4^-$  to p-NP. As result, deposition of silver NPs on the phosphorylated support (Phos-LDH) enables homogeneous dispersion, stabilizes the AgNPs, and maximizes reagent accessibility.

# 5.2. Proposed p-NP reduction mechanism

The proposed 4-NP reduction mechanism shown in Fig. 16 can be summarized as follows: initially, the adsorption of 4-nitrophenol at the surface of the catalyst is achieved thanks to the mutual interaction of the two oxygen atoms of the nitro group with the Ag nanoparticles surface. Afterwards, Transfer of electrons and protons with sodium borohydride (NaBH<sub>4</sub>) acting as a reductant. It delivers hydrogens (protons and electrons) enabling the nitro group of 4-NP to be transformed. The silver nanoparticles promote contact between NaBH<sub>4</sub> and NO $_2^-$ group. Eventually, the nitro group is hydrogenated to an amino group, forming 4-AP. reduction of 4-NP.

### 5.3. Comparative catalytic activity of AgNPs/Phos-LDH

Table 5 shows a comparison between the catalytic performance of the synthesized AgNPs/Phos-LDH and that of a number of other catalysts previously reported in the literature. Since catalytic efficiency is influenced by multiple factors, including catalyst composition, initial concentration, and overall cost, it is often difficult to identify the most effective system. In this context, the synthesized AgNPs/Phos-LDH were evaluated against noble metal-based nanocatalysts as well as other metal oxides and their composites. The results, summarized in Table 5, clearly demonstrate that AgNPs/Phos-LDH offer a more cost-effective, high-yield, and faster alternative while maintaining competitive catalytic activity.

# 6. Conclusion

In conclusion, a layered double hydroxide surface was functionalized with phosphate groups and decorated with silver nanoparticles. The synthesized materials (LDH, Phos-LDH, and AgNPs/Phos-LDH) were thoroughly characterized using XRD, FTIR, SEM-EDS, N2- adsorption/ desorption analysis (BET), and HRTEM. The newly synthesized nanocomposite shows the absence of significant aggregation, indicating good dispersion of AgNPs, thus promoting colloidal stability and preserving their catalytic and antimicrobial activity. The antimicrobial activity of LDH, Phos-LDH, and AgNPs/Phos-LDH nanomaterials were also evaluated. Among them, AgNPs/Phos-LDH exhibited the strongest antimicrobial activity against both bacterial and fungal species, highlighting its potential as an effective antimicrobial agent for biomedical applications. In addition, the developed nanomaterials demonstrated excellent catalytic performance in the reduction of p-nitrophenol to p-aminophenol. Overall, these results underscore the potential of designing alternative catalytic materials that are efficient, stable, and environmentally friendly.

# CRediT authorship contribution statement

Zineb Tchorbo: Writing – review & editing, Writing – original draft.

Marieme Kacem: Writing – review & editing, Writing – original draft,

**Table 5**Summary of reaction conditions and results for the reduction of p-Nitrophenol using diffent catalysts.

Catalyst		Reaction conditions			Results		Ref.
	Catalyst amount (mg)	Reducing agent	Solvent	Temperature (°C)	Time (min)	Conversion (%)	
Fe <sub>3</sub> O <sub>4</sub> /P(GMA-DVB)/ PAMAM/ <b>Au</b>	1	NaBH <sub>4</sub>	Water	r.t	13	99.9	[58]
Pd@PANI-CS-Fe <sub>3</sub> O <sub>4</sub>	1	NaBH <sub>4</sub>	Water	r.t	14	97.8	[59]
3D Co <sub>3</sub> O <sub>4</sub> /NiO	30	NaBH <sub>4</sub>	Water	r.t	10	88	[60]
Pt-Pd nanofibers	5	$H_2$	EtOAc	r.t - 50	240	99	[61]
AgNPs/Phos-LDH	2	NaBH <sub>4</sub>	Water	r.t	6	95	The present work

Note: r.t = room temperature.

Conceptualization. J.M. Doña Rodriguez: Writing – review & editing, Writing – original draft. Meryem Idrissi Yahyaoui: Investigation, Formal analysis, Conceptualization. Abderrahim Essaddek: Writing – review & editing, Supervision, Methodology. Mounsef Neffa: Writing – review & editing, Investigation, Conceptualization. Abdeslam Asehraou: Writing – review & editing, Investigation, Formal analysis, Conceptualization. Mustapha Dib: Writing – review & editing, Writing – original draft, Supervision, Methodology.

# **Declaration of competing interest**

The authors declare that they have no known competing financial interests or personal relationships that could have appeared to influence the work reported in this paper.

### Acknowledgments

The authors would like to thank Mohammed First University of Oujda and the CNRST in Rabat for their partial support of this work. We also express our deep gratitude to Professor R. Quesada Cabrera from the University of Las Palmas de Gran Canaria, Spain, for his invaluable support with the morphological and textural analyses. This work was carried out within the framework of the Erasmus+ project (KA171/2024), and the authors gratefully acknowledge the support provided by the Erasmus+ program.

# Data availability

Data will be made available on request.

# References

- [1] A. Gupta, A. Kirti, R. Narayan Sahu, S.S. Lenka, A. Yadav, A. Choudhury, A. Sinha, A. Nandi, N. Kumar Mohakud, S. Patro, A. Ghosh, N. Kumar Kaushik, M. Suar, S. K. Verma, Translational paradigm in nanodiagnostics applications of functionalized zinc oxide nanoforms interface for pathogenic virus diagnostics, Chem. Eng. J. 509 (2025) 161260, https://doi.org/10.1016/j.cej.2025.161260.
- [2] G.A. Ogunrinola, J.O. Oyewale, O.O. Oshamika, G.I. Olasehinde, The human microbiome and its impacts on health, Microb 7 (2020) 8045646, https://doi.org/ 10.1155/2020/8045646.
- [3] H. Jangid, H. Chandra Joshi, J. Dutta, A. Ahmad, M.B. Alshammari, K. Hossain, G. Aurav Pant, G. Kumar, Advancing food safety with biogenic silver nanoparticles: addressing antimicrobial resistance, sustainability, and commercial viability, F, Chem 26 (2025) 102298, https://doi.org/10.1016/j.fochx.2025.102298.
- [4] J. Qi, T. Zhang, R. Zhang, J. Liu, M. Zong, Q. Zhang, Y. Ping, Y. Gong, B. Zhang, X. Liu, J. Li, X. Wu, B. Li, Fe-doped herbal medicine-based carbon dots nanozyme as safe and effective antimicrobial and wound healing agent, Mater Today Sustain 41 (2024) e01087, https://doi.org/10.1016/j.susmat.2024.e01087.
- [5] R. Qurrat-ul-ain, M. Ur Rahman, H.M. Javed, S. Hassan, T. Munir, R. Asghar, Exploring sulfonamides derivatives Schiff base and metal complexes as antimicrobial agents: a comprehensive review, Inorg. Chem. Commun. 170 (2024) 113396, https://doi.org/10.1016/j.inoche.2024.113396.
- [6] S.E. Abo-Neima, H.A. Motaweh, E.M. Elsehly, Antimicrobial activity of functionalised carbon nanotubes against pathogenic microorganisms, IET Nanobiotechnol. 14 (6) (2020) 0342, https://doi.org/10.1049/iet-nbt.2019.0342.

- [7] A.G. Enderle, I. Franco-Castillo, E. Atrián-Blasco, L. Rafael Martín-Rapún, María J. Lizarraga, M. Culzoni, J.M. de la Bollini, F. Fuente, C. Silva, S. Streb, Cott G. Mitchell, Hybrid antimicrobial films containing a polyoxometalate-ionic liquid, J. ACS Appl. Polym. Mater 4 (6) (2022) 00110, https://doi.org/10.1021/acsapm.2c00110.
- [8] M. Kacem, M. Dib, M.I. Yahyaoui, A. Boussetta, M. Jamil, A. Asehraou, A. Moubarik, A new technology for assembling silylated MgAl-hydrotalcite with a protein derived from shrimp waste to engineer an innovative antimicrobial biocomposite, Inorg. Chem. Commun. 173 (2025) 113894, https://doi.org/ 10.1016/i.inoche.2025.113894.
- [9] X. Sheng-Xue, S. Linyong, Y. Esra, K. Boone, R. Sarikaya, S.K. Vanoosten, A. Misra, Y. Qiang, P. Spencer, T. Candan, Antimicrobial Peptide–Polymer Conjugates For Dentistry, J. Acs Appl. Polym. Mater. 2 (3) (2020) 00921, https://doi.org/10.1021/acsapm.9b00921.
- [10] G. Li, Z. Lai, A. Shan, Advances of antimicrobial peptide-based biomaterials for the treatment of bacterial infections, Adv. Sci. 10 (2023) 2206602, https://doi.org/ 10.1002/advs.202206602.
- [11] S.A.A. Mohamed, S.D. Mekkey, A.M. Othman, M. El-Sakhawy, Novel antimicrobial biodegradable composite films as packaging materials based on shellac/chitosan, and ZnAl<sub>2</sub>O<sub>4</sub> or CuAl<sub>2</sub>O<sub>4</sub> spinel nanoparticles, Sci. Rep. 14 (1) (2024) 27824, https://doi.org/10.1038/s41598-024-78261-1.
- [12] M.C. Ristina Furlaneto, L. Furlaneto-Maia, Antimicrobial nanoparticle-containing food packaging films for controlling Listeria spp: an overview, J. Food Microb. (2024) 110959, https://doi.org/10.1016/j.ijfoodmicro.2024.110959.
- [13] A.I. El-Batal, M.I. Eisa, M.A. Saad, H.M. Fakhry, W.M. El-Neshwy, S.S. Abdel-Fatah, F.M. Mosallam, G.S. El-Sayyad, Gum Arabic assisted the biomass synthesis of bimetallic silver copper oxide nanoparticles using gamma-rays for improving bacterial and viral wound healing: promising antimicrobial activity against foot and mouth disease, J. Bio. Macro 262 (2024) 130010, https://doi.org/10.1016/j.ijbiomac.2024.130010.
- [14] F. Rizzi, E. Fanizza, M. Giancaspro, N. Depalo, M.L. Curri, B. González, M. Colilla, I. Izquierdo-Barba, M. Vallet-Regí, Mesoporous silica nanostructures embedding NIR active plasmonic nanoparticles: Harnessing antimicrobial agents delivery system for photo-assisted eradicating Gram-positive bacteria, Microporous Mesoporous Mater. 383 (2025) 113414, https://doi.org/10.1016/j.micromeso.2024.113414.
- [15] A.S. Rodrigues, J.G. Batista, M.Á. Rodrigues, V.C. Thipe, L.A. Minarini, P.S. Lopes, A.B. Lugão, Advances in silver nanoparticles: a comprehensive review on their potential as antimicrobial agents and their mechanisms of action elucidated by proteomics, Front. Microbiol. 15 (2024) 1440065, https://doi.org/10.3389/ fmicb.2024.1440065.
- [16] T.C. Prathna, N. Chandrasekaran, A. Mukherjee, Studies on aggregation behaviour of silver nanoparticles in aqueous matrices: effect of surface functionalization and matrix composition, Colloids Surf. A Physicochem. Eng. Asp. 390 (1–3) (2011) 216–224, https://doi.org/10.1016/j.colsurfa.2011.09.047.
- [17] J. Lutz, K. Albrecht, J. Groll, Thioether-polymer coating for colloidal stabilization of silver nanoparticles, Adv. NanoBiomed Res. 1 (2021) 2000074, https://doi.org/ 10.1002/aphr.202000074
- [18] P. Cyganowski, A. Dzimitrowicz, M.M. Marzec, S. Arabasz, K. Sokołowski, A. Lesniewicz, S. Nowak, P. Pohl, A. Bernasik, D. Jermakowicz-Bartkowiak, Catalytic reductions of nitroaromatic compounds over heterogeneous catalysts with rhenium sub-nanostructures, Sci. Rep. 13 (2023) 12789, https://doi.org/ 10.1038/s41598-023-39830-y.
- [19] J. Zhao, R. Jin, Heterogeneous catalysis by gold and gold-based bimetal nanoclusters, Nanotoday 18 (2018) 86–102, https://doi.org/10.1016/j. nantod.2017.12.009.
- [20] N.A. Tajuddin, E.F.B. Sokeri, N.A. Kamal, M. Dib, Fluoride removal in drinking water using layered double hydroxide materials: preparation, characterization and the current perspective on IR4. 0 technologies, J. Environ. Chem. Eng. 11 (3) (2023) 110305, https://doi.org/10.1016/j.jecc.2023.110305.
- [21] A. Laksir, M. Kacem, M. Dib, R. Touzani, A. Boulouiz, MOFs-based materials: a trendy hybrid catalyst for hydrogenation of aromatic nitro compounds, Interactions 246 (2025) 18, https://doi.org/10.1007/s10751-024-02242-z.
- [22] S. Akhramez, Y. Achour, M. Dib, L. Bahsis, H. Ouchetto, A. Hafid, M. Khouili, El Haddad, M, DFT study and synthesis of novel bioactive bispyrazole using Mg/Al-

- LDH as a solid base catalyst, Curr. Chem. Biol. 14 (4) (2020) 240–249, https://doi.org/10.2174/2212796814999200918175018.
- [23] M. Xu, M. Wei, Layered double hydroxide-based catalysts: recent advances in preparation, structure, and applications, Adv. Funct. Mater. 28 (2018) 1802943, https://doi.org/10.1002/adfm.201802943.
- [24] S. Talbi, M. DiD, L. Bouissane, H. Abderrafia, S. Rabi, M. Khouili, Recent Progress in the Synthesis of heterocycles based on 1,3-diketones, Curr. Org. Synth. 19 (2022) 220–245, https://doi.org/10.2174/1570179418666211011141428.
- [25] K. ElFarouki, M. Kacem, M. Dib, H. Ouchetto, A. Hafid, M. Khouili, A review on the recent Progress of layered double hydroxides (LDHs)-based catalysts for heterocyclic Synthesis, Curr. Organocatal. 11 (2024) 154–174, https://doi.org/ 10.2174/0122133372264682231019101634.
- [26] T. Hu, Z. Gu, G.R. Williams, M. Strimaite, J. Zha, Z. Zhou, X. Zhang, C. Tan, R. Liang, Layered double hydroxide-based nanomaterials for biomedical applications, Chem. Soc. Rev. 51 (14) (2022) 6126–6176, https://doi.org/ 10.1039/D2CS00236A.
- [27] A. Singha Roy, S. Kesavan Pillai, S.S. Ray, Layered double hydroxides for sustainable agriculture and environment, ACS Omega 7 (24) (2022) 20428–20440, https://doi.org/10.1021/acsomega.2c01405.
- [28] K. Fan, P. Xu, Z. Li, M. Shao, X. Duan, Layered double hydroxides: next promising materials for energy storage and conversion, Next Mater 1 (4) (2023) 100040, https://doi.org/10.1016/j.nxmate.2023.100040.
- [29] M. Dib, M. Kacem, N.A. Tajuddin, Recent progress in layered double hydroxides-based materials as sustainable nanoadsorbents for hazardous pollutants recovery from aqueous medium, Curr. Mater. Sci 18 (1) (2025) 76–97, https://doi.org/10.2174/2666145417666230914104249.
- [30] R. Sharma, G.G.C. Arizaga, A.K. Saini, P. Shandilya, Layered double hydroxide as multifunctional materials for environmental remediation: from chemical pollutants to microorganisms, Sustain. Mater. Technol. 29 (2021) 00319, https://doi.org/ 10.1016/j.susmat.2021.e00319.
- [31] K. Elfarouki, B. Chhaibi, S. Aghris, M. Kacem, S. Lahrich, M. Abderrahim EL Mhammedi, M. Dib, A. Hafid, M. Khouili, Electrochemical sensor based on CoMgFe-trimetallic layered double hydroxides for Flubendiamide detection in water samples, J. Electrochem. Soc. 172 (1) (2025) 017515, https://doi.org/10.1149/1945-7111/adaa28.
- [32] W. Lv, Q. Mei, H. Fu, J. Xiao, M. Du, Q. Zheng, A general strategy for the synthesis of layered double hydroxide nanoscrolls on arbitrary substrates: its formation and multifunction, J. Mater. Chem. A.5.36 (2017) 19079–19090, https://doi.org/ 10.1039/C7TA05556K
- [33] V. Kovalenko, V. Kotok, B. Murashevych, Layered double hydroxides as the unique product of target ionic construction for energy, chemical, foods, cosmetics, medicine and ecology applications, Chem. Rec. 24 (2) (2024) 202300260, https:// doi.org/10.1002/tcr.202300260.
- [34] S.K. Mondal, S. Chakraborty, S. Manna, S.M. Mandal, Antimicrobial nanoparticles: current landscape and future challenges, RSC Pharmaceut. 1 (3) (2024) 00032, https://doi.org/10.1039/D4PM00032C.
- [35] S. Kotta, H. Mubarak Aldawsari, N.A. Alhakamy, M. Abdelkhalek Elfaky, S. M. Badr-Eldin Synthesis, Structural characterization, and antimicrobial evaluation of silver nanoparticle-embedded layered double hydroxides for delivery in polymeric hydrogel matrices, J. Pharm. Innov. 19 (2024) 09901, https://doi.org/10.1007/s12247-024-09901-2.
- [36] M. Kacem, N. Katir, J. El Haskouri, A. Essoumhi, El Kadib, Gold nanoparticles grown on a hydrophobic and texturally tunable PDMS-like framework, New J. Chem. 45 (2021) 10232–10239, https://doi.org/10.1039/D1NJ00274K.
- [37] M. Dib, H. Ouchetto, S. Akhramez, H. Fadili, A. Essoumhi, K. Ouchetto, M. Sajieddine, M. Khouili, Preparation of Mg/Al-LDH nanomaterials and its application in the condensation of 3-amino-1-phenyl-2-pyrazolin-5-one with aromatic aldehyde, Mater Today Proc 22 (2020) 104–107, https://doi.org/ 10.1016/j.matpr.2019.08.106.
- [38] M. Dib, M.N. Bennani, H. Ouchetto, K. Ouchetto, A. Hafid, M. Khouili, Effect of exchanged MgAl-hydrotalcite with carbonate on increases of acid neutralizing capacity: a good candidate as an antacid, Curr. Nanomater 7 (2022) 49–56, https://doi.org/10.2174/2405461506666210526145531.
- [39] J.Y. He, D. Zhang, X.J. Wang, J. Zhao, Y.P. Li, Y. Liu, F.T. Li, Phosphorylation of NiAl-layered double hydroxide nanosheets as a novel cocatalyst for photocatalytic hydrogen evolution, Int. J. Hyd. Energy 46 (36) (2021) 18977–18987, https://doi. org/10.1016/j.ijhydene.2021.03.064.
- [40] M. Haddou, A. Elbouzidi, M. Taibi, A. Baraich, R. El Hassania Loukili, E. Bellaouchi, A. Saalaoui, A. Mohammad Asehraou, M. Bourhia Salamatullah, Hiba-Allah Nafidi, M. Hamed Addi, B. El Guerrouj, K. Chaabane, Exploring the multifaceted bioactivities of Lavandula pinnata L. essential oil: promising pharmacological activities, Front. Chem. 12 (2024) 1383731, https://doi.org/ 10.3389/fchem.2024.1383731.
- [41] A. Elbouzidi, M. Taibi, S. Laaraj, E.H. Loukili, M. Haddou, N. El Hachlafi, H. Naceiri Mrabti, A. Baraich, R. Bellaouchi, A. Asehraou, M. Bourhia, H.A. Nafidi, Yo.A. Bin Jardan, K. Chaabane, Chemical profiling of volatile compounds of the essential oil of grey-leaved rockrose (Cistus albidus L.) and its antioxidant, antiinflammatory, antibacterial, antifungal, and anticancer activity in vitro and in silico, M. Addi, Front. Chem. 12 (2024) 1334028, https://doi.org/10.3389/ frhem.2024.1334028.
- [42] M. Taibi, A. Elbouzidi, M. Haddou, E.H. Loukili, R. Bellaouchi, A. Asehraou, Y. Douzi, M. Addi, A.M. Salamatullah, H.-A. Nafidi, Chemical profiling, antibacterial efficacy, and synergistic actions of Ptychotis verticillata Duby essential oil in combination with conventional antibiotics, Nat. Prod. Commun. 19 (2024) 1, https://doi.org/10.1177/1934578X231222785.

- [43] S.P. Newman, W. Jones, Synthesis, characterization and applications of layered double hydroxides containing organic guests, New J. Chem. 22 (2) (1998) 708319, https://doi.org/10.1039/A708319J.
- [44] Y. Sui, X. Liu, S. Bai, X. Li, Z. Sun, Phosphate loaded layered double hydroxides for active corrosion protection of carbon steel, corrosion engineering, Sci. Technol. 57 (1) (2022) 1976086, https://doi.org/10.1080/1478422X.2021.1976086.
- [45] N.A. Kamal, N.H. Pungot, S.K. Che Soh, N.A. Tajuddin, Facile and green hydrothermal synthesis of MgAl/NiAl/ZnAl layered double hydroxide nanosheets: a physiochemical comparison, Pure Appl. Chem. 96 (11) (2024) 0014, https://doi. org/10.1515/pac-2024-0014.
- [46] R. Gogoi, M. Baruah, A. Borgohain, J. Saikia, V. Jyoti Baruah, S. Rohman, M. Singh, R. Kar, S.K. Dey, B. Mazumder, T. Karak, Intercalation vs adsorption strategies of Myo inositol Hexakisphosphate into Zn-Fe layered double hydroxide: a Tiff between anion exchange and coprecipitation, ACS Omega 8 (2023) 43151–43162, https://doi.org/10.1021/acsomega.3c06788.
- [47] X. Chen, H. Wang, B. Xia, R. Meng, Noncovalent phosphorylation of CoCr layered double hydroxide nanosheets with improved electrocatalytic activity for the oxygen evolution reaction, Chem. Commun. 55 (80) (2019) 06863, https://doi. org/10.1039/C9CC06863E.
- [48] C. Chen, P. Gunawan, X.W. Lou, R. Xu, Silver nanoparticles deposited layered double hydroxide nanoporous coatings with excellent antimicrobial activities, Adv. Funct. Mater. 22 (4) (2012) 201102333, https://doi.org/10.1002/ adfm 201102333
- [49] Y. Wang, S. Luo, Z. Wang, Y. Fu, Structural and textural evolution of nanocrystalline Mg-Al layered double hydroxides during mechanical treatment, Appl. Clay Sci. 80 (2013) 334–339, https://doi.org/10.1016/j.clay.2013.05.015.
- [50] S.K. Bhagat, A.S. Nagpure, M.R. Lanjewar, N.G. Gode, S.R. Thakare, Investigation of structural and morphological insights of nanostructured layered double hydroxides: catalytic activity in aldol condensation, J. Por. Maters 31 (2) (2024) 759–778, https://doi.org/10.1007/s10934-023-01545-w.
- [51] B. Kowalska-Krochmal, R. Dudek-Wicher, The minimum inhibitory concentration of antibiotics: methods, interpretation, clinical relevance, Pathogens 10 (2) (2021) 10020165, https://doi.org/10.3390/pathogens10020165.
- [52] L. Li, I. Soyhan, E. Warszawik, P. van Rijn, Layered double hydroxides: recent Progress and promising perspectives toward biomedical applications, Adv. Sci. 11 (2024) 2306035, https://doi.org/10.1002/advs.202306035.
- [53] D. Pattappan, S. Kapoor, S. Safiul Islam, Yi-Ting Lai, Layered double hydroxides for regulating phosphate in water to achieve long-term nutritional management, ACS Omega 8 (28) (2023) 24727–24749, https://doi.org/10.1021/acsomega.3c02576.
- [54] L.D.S. Missio Pinheiro, G.G. Sangoi, B. Stefanello Vizzotto, Y.P. Moreno Ruiz, A. Galembeck, G. Pavoski, D.C.R. Espinosa, A. Kolinski Machado, W.L.O. da Silva, Silver nanoparticles from ascorbic acid: biosynthesis, characterization, in vitro safety profile, antimicrobial activity and phytotoxicity, Mater. Chem. Phys. 325 (2024) 129715, https://doi.org/10.1016/j.matchemphys.2024.129715.
- [55] L.B. de Menezes, D.M. Druzian, L. Rodrigues Oviedo, G.K. Cossettin Bonazza, A. Kolinski Machado, W., Leonardo da Silva, in vitro safety profile and phytoecotoxicity assessment of the eco-friendly calcium oxide nanoparticles, Chemosphere 365 (2024) 143407, https://doi.org/10.1016/j. chemosphere.2024.143407.
- [56] L.F. Wentz Brum, M.D. Costa Rodrigues da Silva, C. dos Santos, G. Pavoski, D.C. Romano Espinosa, W. Leonardo da Silva, Green synthesis of niobium (V) oxide nanoparticles using pecan nutshell (Carya illinoinensis) and evaluation of its antioxidant activity, Catal. Today 445 (2025) 115106, https://doi.org/10.1016/j.cost/10.1016/j.
- [57] X. Gong, N.D. Jadhav, V.V. Lonikar, A.N. Kulkarni, H. Zhang, B.R. Sankapal, J. Ren, B.B. Xu, H.M. Pathan, Y. Ma, Z. Lin, E. Witherspoon, Z. Wang, Z. Guo, An overview of green synthesized silver nanoparticles towards bioactive antibacterial, Antimicrobial. Antifungal Appl. Adv. Coll. Inter. Sci. 323 (2024) 103053, https:// doi.org/10.1016/j.cis.2023.103053.
- [58] M. Ma, Y. Yang, W. Li, R. Feng, Z. Li, P. Lyu, Y. Ma, Gold nanoparticles supported by amino groups on the surface of magnetite microspheres for the catalytic reduction of 4-nitrophenol, J. Mater. Sci. 54 (2019) 323–334, https://doi.org/ 10.1007/s10853-018-2868-1.
- [59] M.M. Ayad, Wael A. Amer, M.G. Kotp, Magnetic polyaniline-chitosan nanocomposite decorated with palladium nanoparticles for enhanced catalytic reduction of 4-nitrophenol, Mol. Catal. 439 (2017) 72–80, https://doi.org/ 10.1016/j.mcat.2017.06.023.
- [60] A. Chinnappan, S.K. Eshkalak, C. Baskar, M. Khatibzadeh, E. Kowsarid, S. Ramakrishna, Flower-like 3-dimensional hierarchical Co3O4/NiO microspheres for 4-nitrophenol reduction reaction, Nanoscale Adv 1 (2019) 305–313, https:// doi.org/10.1039/C8NA00029H.
- [61] M. Takasaki, Y. Motoyama, K. Higashi, I. Seong-Ho Yoon, H.Nagashima Mochida, Chemoselective hydrogenation of nitroarenes with carbon nanofiber-supported platinum and palladium nanoparticles, Org. Lett. 10 (2008) 1601–1604, https:// doi.org/10.1021/ol800277a.



Zineb Tchorbo is a PhD student at Mohammed Premier University, Oujda, Morocco. She obtained her Master's degree in Physiochemistry of Materials from the Faculty of Sciences at the same university. Her research focuses on layered double hydroxides modified with phosphate compounds for catalytic and environmental applications, under the supervision of Prof. Abderrahim Essaddek and Prof. Mustapha Dib. She is also interested in the development of sustainable materials for innovative applications.



Mustapha Dib (born October 9, 1987, in Morocco) obtained his PhD in inorganic chemistry and catalysis from the Faculty of Science and Technology at Sultan Moulay Slimane University (Beni Mellal, Morocco), under the supervision of Professor Hajiba Ouchetto. He had previously obtained a master's degree in materials and applied catalysis at the Faculty of Sciences of Moulay Ismail University in Meknes. He is currently an associate professor at the Faculty of Sciences of Mohammed Premier University (Oujda, Morocco). His research focuses on the synthesis of functional materials and nanomaterials, with a particular focus on their catalytic properties and environmental applications. His work aims to address current global chal-

lenges through the design of innovative materials and sustainable magnetic nanocomposites for biological applications. Dr. DIB Mustapha has participated as a member of scientific committee for several international conferences and he is reviewer for various scientific journals.